We believe that rf water plasma treatment may be a generally applicable method for preparing model, hydroxylated metal oxide surfaces. Future investigations concerned with the interaction of water plasmas with a variety of metal oxide surfaces are warranted to determine if the effects described here for tin oxide surfaces can be extended to other systems and, perhaps, generalized.

Acknowledgment. This research was supported by the National Science Foundation.

Registry No. H_2O, 7732-18-5; SnO_2, 18282-10-5.

Structural and Magnetic Characterization of α- and β-4,4'-(Butadiyne-1,4-diyl)bis(2,2,6,6-tetramethyl-4-hydroxypiperidin-1-oxyl) and Characterization of Its Thermal Degradation Product†

Joel S. Miller,*[1a] Daniel T. Glatzhofer,[1a,b] Rene Laversanne,[1b] Thomas B. Brill,*[1c] Mark D. Timken,[1c] Charles J. O'Connor,*[1d] Jian H. Zhang,[1d] Joseph C. Calabrese,[1a] Arthur J. Epstein,*[1b] Sailesh Chittipeddi,[1b] and Patricia Vaca[1b]

Central Research and Development, E. I. du Pont de Nemours and Co., Inc., Experimental Station 328, Wilmington, Delaware 19880-0328, Department of Physics and Department of Chemistry, The Ohio State University, Columbus, Ohio 43210-1106, Department of Chemistry, University of Delaware, Newark, Delaware 19716, and Department of Chemistry, University of New Orleans, New Orleans, Louisiana 70148

Received October 26, 1989

A new polymorph of 4,4'-(butadiyne-1,4-diyl)bis(2,2,6,6-tetramethyl-4-hydroxypiperidin-1-oxyl), 1, has been prepared. Both phases have been characterized by X-ray diffraction, infrared and Raman spectroscopies, and magnetic susceptibility. The α-phase belongs to the *Pccn* space group [a = 19.049 (4) Å, b = 16.107 (4) Å, and c = 14.113 (3) Å, V = 4330 (3) Å^3, Z = 8, T = −115 °C, R_u = 7.0%, R_w = 8.0%] and the β-phase belongs to the $Pca2_1$ space group [a = 14.265 (1) Å, b = 8.079 (3) Å, and c = 18.865 (2) Å, V = 2174.1 Å^3, Z = 4, T = −100 °C, R_u = 4.8%, R_w = 5.0%]. The molecular structures of both phases are essentially equivalent with the average C≡C, CC—CC, and NO distances of 1.200, 1.385, and 1.288 Å, respectively. The hydrogen bonding OH···ON (or O···O) interactions [i.e., 1.70 (2.834) and 1.72 Å (2.757 Å) for the α-phase and 1.85 (2.804) and 1.84 Å (2.788 Å) for the β-phase] are the only significant intermolecular interactions. Intense ν_{NO} and $\nu_{C\equiv C}$ (Raman) vibrations occur at 1341 and 2236 cm^{-1}, respectively, for both phases. A pleated sheet and helical, hydrogen-bonded solid-state motifs are observed for the α- and β-phases, respectively. On the basis of accepted structural criteria, both solid-state structures should not support single-crystal topochemical polymerization and UV, electron beam, and γ-ray induced polymerization has not been achieved for either phase. Thermal treatment, however, turns the crystals black. Thermogravimetric analysis under nitrogen reveals an explosive decomposition at ~140 °C for both phases. Thermal decomposition monitored by FTIR reveals the loss of the nitroxyl group, destruction of the ring system, and formation of small molecules and a residue more complex than that expected for a simple polymerization. The SQUID magnetic susceptibility of both phases obey the Curie–Weiss expression with θ = ~−1.8 K. The effective moment is ~2.45 μ_B per molecule, which is consistent with two independent $S = {}^1/_2$ spins per molecule. Analysis of the exchange narrowing of the ESR line of α- and β-phases led to an intermonomer exchange of J ~0.165 K (0.115 cm^{-1}). Application of the Weiss molecular field model for the measured $|\theta|$ of ~1.8 K leads to an estimate of ~0.155 K (0.108 cm^{-1}) for the intermonomer exchange J, in very good agreement with the estimate derived from ESR. Upon thermal treatment (~20 h at 80–100 °C) of either phase, a resultant black material forms that exhibit a reduced susceptibility corresponding to <1 μ_B per monomer and nearly zero Curie–Weiss temperature, θ. EPR studies of the thermal degradation products show a complex pattern characteristic of isolated $S = {}^1/_2$ spins interacting with the S = 1 nitrogen nuclear spin and broadened by the dipole interactions with the nearby proton spins. Study of the temperature-dependent EPR of dilute solutions of 1 confirms this analysis and suggests that the majority of the residual spins remaining after heat treatment are monoradicals. The temperature dependence of the intensity of triplet EPR observed for the heat-treated samples suggests the presence of a triplet-exchange interaction of $J_{triplet}$ ~ 10 K. The static and dynamic magnetic data of the thermal degradation products do not provide any evidence for significant 3-D ferromagnetism or even magnetic coupling and indicate the presence of only very weak intradimer ferromagnetic (triplet) coupling.

Introduction

The quest for a molecular-based ferromagnet has culminated with the characterization of decamethylferrocenium tetracyanoethenide, $[Fe^{III}(C_5Me_5)_2]^{\bullet+}$-$[TCNE]^{\bullet-}$, as having bulk ferromagnetic behavior.[2,3] The search for ferromagnetic organic compounds and polymers, however, continues to be of interest.[3-7] Reports of ferromagnetic polymeric materials have been plagued by ill-defined compositions, low yields, lack of characteriza-

† Contribution No. 5024 from E. I. du Pont de Nemours and Company.

(1) (a) E. I. du Pont de Nemours and Co., Inc. (b) The Ohio State University. (c) University of Delaware. (d) University of New Orleans.

(2) Miller, J. S.; Calabrese, J. C.; Bigelow, R. W.; Epstein, A. J.; Zhang, R. W.; Reiff, W. M. *J. Chem. Soc., Commun.* **1986**, 1026–1028. Miller, J. S.; Calabrese, J. C.; Rommelmann, H.; Chittipeddi, S.; Zhang, R. W.; Reiff, W. M.; Epstein, A. J. *J. Am. Chem. Soc.* **1987**, *109*, 769–781. Chittapeddi, S.; Cromack, K.; Miller, J. S.; Epstein, A. J. *Phys. Rev. Lett.* **1987**, *58*, 2695.

0897-4756/90/2802-0060$02.50/0

Scheme I

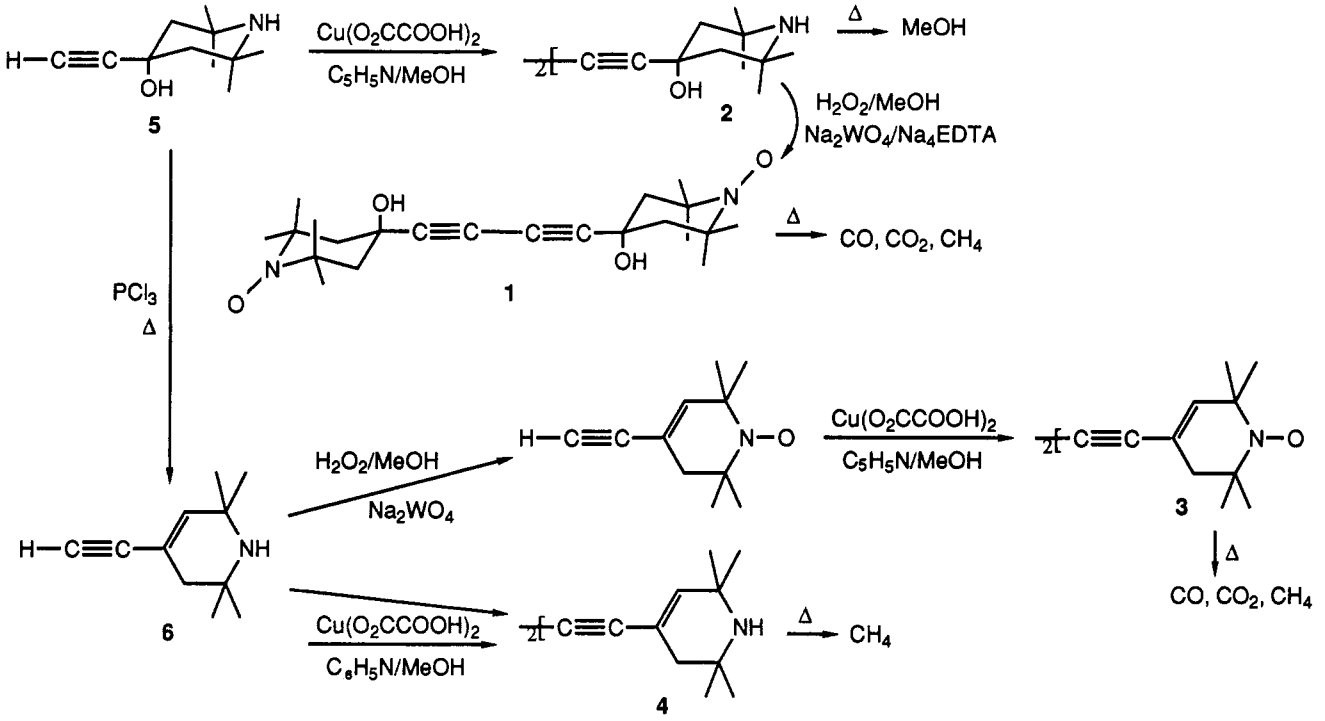

tion, and poor reproducibility.[6,7] Ovchinnikov and co-workers have recently reported the thermal, photochemical, and glow discharge treatment of 4,4′-(butadiyne-1,4-diyl)bis(2,2,6,6-tetramethyl-4-hydroxypiperidin-1-oxyl), **1**,

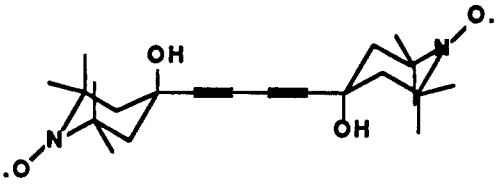

1

to form a black polymer of which some samples exhibit field-dependent magnetization corresponding to an "insignificant" amount (0.1%) of a ferromagnet.[7a,b] Furthermore, Cao and co-workers report a magnetization that corresponds to 0.7% of the sample being a ferromagnet.[7d] This chemistry attempts to take advantage of the fact that some diacetylenes crystallize in such a manner that enables thermal, photochemical, or X-ray induced topochemical polymerization to form a single-crystal polymer or polydiacetylenes in a single-crystal matrix.[8] Due to the arrangement of the diacetylenes, the orthorhombic *Pccn* structure (i.e., α-phase) of the monomer is unfavorable[7b,c] for single-crystal topochemical polymerization.

As part of our continued interest in molecular-based ferromagnetic materials,[2,3] we have prepared **1** in an effort to verify and elucidate its ferromagnetic behavior after thermal or γ-ray treatment and have characterized a new but similar polymorph, i.e., β-phase, of the monomer. Unlike the "perfect needle" crystal[7b] habit for the α-phase, the β-phase forms orange parallelpiped crystals that are also orthorhombic. Herein we report the detailed crystal structures and magnetic and thermal properties of the α- and β-phases.

Experimental Section

4,4′-(Butadiyne-1,4-diyl)bis(2,2,6,6-tetramethyl-4-hydroxypiperidin-1-oxyl), **1**, was synthesized by oxidation of the corresponding bis(piperidine), **2**, with hydrogen peroxide and a sodium pertungstate/tetrasodium ethylenediaminetetraacetate catalyst (Scheme I).[9] Crystals of the α-phase were obtained from a solution of pure **1** dissolved in a minimal amount of methanol at room temperature followed by rapid addition of 2.5 volumes of distilled water and allowing the solution to stand undisturbed several hours. Orange parallelpiped crystals of the β-phase were reproducibly obtained by slow recrystallization of **1** from either hot ethyl acetate or methanol. Both materials were collected by filtration and dried under reduced pressure. Anal. Calcd for $C_{22}H_{34}N_2O_4$: C, 67.66; H, 8.78; N = 7.17. Found for the α-phase: C, 67.79; H, 8.88; N, 7.09. Found for the β-phase: C, 67.78; H, 8.84; N, 7.19. IR (KBr pellet) ν_{OH} = 3360 s, ν_{NO} = 1341 s, and Raman $\nu_{C\equiv C}$ = 2236 s cm^{-1}. For the bis(piperidine) starting material, **2**: IR (KBr pellet) $\nu_{OH,NH}$ = 3289, 3070 s, 3021, and Raman $\nu_{C\equiv C}$ = 2245 s cm^{-1}.

Diradical **3** and its bis(piperidine) precursor **4** were prepared according to the literature[10] with the exceptions that the reaction to form enyne **6** was carried out in neat phosphorus oxychloride

(3) Miller, J. S.; Epstein, A. J. *J. Am. Chem. Soc.* **1987**, *109*, 3850. Miller, J. S.; Epstein, A. J.; Reiff, W. M. *Chem. Rev.* **1988**, *88*, 201, Miller, J. S.; Epstein, A. J. *NATO ASI* **1987**, *168B*, 159–174. Miller, J. S.; Epstein, A. J.; Reiff, W. M. *Acc. Chem. Res.* **1988**, *23*, 114.

(4) Itoh, K.; Takai, K. *Mol. Cryst. Liq. Cryst.* **1985**, *125*, 251. Iwamura, H. *Pure App. Chem.* **1986**, *58*, 187.

(5) Breslow, R. *Mol. Cryst. Liq. Cryst.* **1985**, *125*, 261–267.

(6) Torrance, J. B.; Oostra, S.; Nazzal, *Synth. Met.* **1987**, *19*, 708. Torrance, J. B.; Bagus, P. S.; Johannsen, I.; Nazzal, A.; Parkin, S. S. P.; Batail, P. *J. Appl. Phys.* **1988**, *63*, 2962–2965.

(7) (a) Korshak, Yu. V.; Ovchinnikov, A. A.; Shapiro, A. M.; Medvedeva, T. V.; Specktor, V. N. *Pisma Zh. Eksp. Teor. Fiz.* **1986**, *43*, 309–311. (b) Korshak, Yu. V.; Medvedeva, T. V.; Ovchinnikov, A. A.; Specktor, V. N. *Nature* **1987**, *326*, 370–372. (c) Buchachenko, A. L.; Shibaeva, R. P.; Rozenberg, L. P.; Ovchinnikov, A. A. *Khim. Phys.* **1987**, *6*, 773–778. (d) Cao, Y.; Wang, P.; Hu, Z.; Ki, S.; Zhang, L.; Zhao, J. *Solid State Commun.* **1988**, *68*, 817; *Synth. Met.* **1988**, *27*, B625. (e) Miller, J. S.; Epstein, A. J.; Glatzhofer, D. T.; Calabrese, J. C. *J. Chem. Soc., Chem. Commun.* **1988**, 322.

(8) Bassler, H. *Adv. Polym. Sci.* **1984**, *63*, 1–48. Baughman, R. H.; Chance, R. R. *Ann. N.Y. Acad. Sci.* **1978**, *313*, 705–725. Bloor, D.; Chance, R. R. Polydiacetylenes. *NATO ASI, Ser. E, No.* **1985**, *102*.

(9) Rozantzev, E. G. *Free Nitroxy Radicals*; Plenum: New York, 1970; pp 227–228.

(10) (a) Paulikov, V. V.; Shapiro, A. B.; Rozantzev, E. G. *Izv. Akad. Nauk. SSSR, Ser. Khim.* **1980**, 128–132. (b) Shapiro, A. B.; Skripnichenko, L. N.; Paulikov, V. V.; Rozantzev, E. G. *Izv. Akad. Nauk. SSSR, Ser. Khim.* **1979**, 151–158.

and reflux was continued only until all starting alcohol 5 had just disappeared (45% yield). Both 3 and 4 gave satisfactory elemental analyses.

X-ray Data Collection and Data Reduction. After the initial report of the cell constants and space group of the α-phase,[7b] we isolated the β-phase.[7e] Since the lattice parameters of α- and β-phases differed by only $b_\alpha \approx 2b_\beta$, we verified that β-phase was correctly determined by X-ray diffraction (vide infra). With only minimal information available on the α-phase we wanted to verify that it was not mistaken for the β-phase, and thus its structure was determined in our laboratory. Recently the structure of the α-phase has been described;[7c] however, due to a greater reflections/parameter ratio, lower temperature (−115 °C vs room temperature), uncertainty of the R value, and the lack of individual esd's, we report our results and summarize the differences between these phases. The relevant conditions of data collection, data reduction, and structure refinement are summarized in Table S1 (supplementary material; see the paragraph at the end of the paper). Since the lattice parameters of $Pccn$ α- and the $Pca2_1$ β-phases differ by $a_\alpha \approx c_\beta$, $c_\alpha \approx a_\beta$, and $b_\alpha \approx 2b_\beta$, we verified that the room-temperature unit-cell parameters of the β-phase [α = 14.390 (2) Å, b = 8.168 (1) Å, and c = 18.720 (1) Å, V = 2200.3 Å^3] are slightly greater than those at −100 °C as expected for thermal contraction. Upon collection of a suitable partial data set (0–15°) using b_α (i.e., $2b_\beta$), we did not observe any reflections with odd values for the k Miller index, which verified our choice of b_β. Additionally, an exhaustive review of the film data did not reveal evidence that β should be doubled to that noted for the α-phase. The refinement of the β-phase is hampered by a noncrystallographic inversion center within the molecule, with high parameter correlations (maximum correlation coefficient of 0.88), and leads to an increased dispersion for chemically equivalent bond distances. However, the centric equivalent ($Pcam$) is effectively ruled out by the molecular orientation with respect to the c-axis mirror. There were no apparent phase solutions using the centric symmetry.

Magnetic Susceptibility. Magnetic data were recorded by using several independent facilities and techniques. A S.H.E. Corp. VTS superconducting SQUID susceptometer was used to obtain susceptibility from samples heat treated in situ. The sample bucket was fabricated from an Al–Si alloy obtained from S.H.E. Corp. The magnetic susceptibility of the sample bucket was measured independently between 6 and 300 K at 1 kG, and the susceptibility data for all samples were then corrected for the bucket contribution. The field dependence of the magnetization of the samples after thermal treatment was measured at temperatures of 6, 30, and 90 K. The magnetization data were corrected for the bucket contribution, which was obtained at the same temperature between 0.1 and 50 kG. Calibration and measurement procedures are reported elsewhere.[11] Independent magnetic susceptibility and field-dependent magnetization measurements taken at Ohio State[12a] and Du Pont[12b] were determined by the Faraday method using systems as previously described.

Electron Paramagnetic Resonance. Temperature-dependent EPR spectra were reported on either a IBM/Brüker ER 200 D-SRC or a Bruker 300 D spectrometer operating at at 9.6 GHz using an Oxford EPR-9 temperature controller.

Sample Treatment. Ultraviolet irradiation of samples was carried out with a spiral mercury arc lamp (2 h) or Rayonet photochemical reactor (ca. 300-nm peak output, 4 h). Prolonged exposures (6–48 h) were carried out by irradiating the samples under a Mineralight Model UVSL-58 lamp with the filter removed. γ-ray irradiation (2 Mrad) from a ^{60}Co source was carried out by Neutron Products Inc., Dickerson, MD, and and electron beam irradiation (5 Mrad) was performed by Electron Technologies Corp., South Windsor, CT. In all cases sample temperatures did not exceed 60 °C.

Thermal treatment of α-phase for Faraday susceptibility studies at Du Pont and OSU were carried out either in a Pyrex tube sealed under vacuum or in a quartz tube under N_2 atmosphere. The sample in the sealed tube was heated at temperatures of 80–85 °C for 20 h in a tube furnace with temperature controller. The sample under N_2 atmosphere was heated at temperature of 95–100 °C for 20 h in a heating bath. Thermal treatment of β-phase samples intended for similar studies was carried out at 95–100 °C for 20 h in a quartz tube under nitrogen.

Alternatively, thermal treatment of the α- or β-phases was either carried out in the respective apparatus using appropriate heating devices or independently by placing the samples in quartz ESR tubes that were evacuated, placed under a slight positive N_2 pressure, and then placed in a heating bath at the desired temperature. After the designated time, the tubes were taken from the bath and allowed to cool, and the samples were removed for analysis. All handling of the materials, before and after thermal treatment, was carried out using Teflon-coated or plastic utensils, and extreme care was taken to minimize exposure to other external sources of ferromagnetic impurities such as dust.

Thermal treatment for the SQUID measurements on both α- and β-phases was performed at 95–100 °C for 20 h under nitrogen. To minimize exposure to other external sources of ferromagnetic impurities, great care was taken in handling the sample. During our sample manipulations, the sample came into contact only with glass utensils and/or the Si/Al alloy SQUID sample bucket. The magnetic susceptibility of the α-phase was recorded with the sample in the SQUID bucket suspended from a cotton fiber. After the susceptibility was measured as a function of temperature, the holder containing sample was suspended in a quartz tube which was placed in a heating bath for thermal treatment. After thermal treatment, the holder with sample was immediately placed into the SQUID for susceptibility and magnetization measurements. Only the cotton thread was handled during the sample manipulations following initial magnetic measurement of the fresh specimen.

Physical Measurements. IR and Raman spectra were recorded on a Perkin-Elmer 283B spectrometer and a Bomem DA3 interferometer modified to do near-infrared FTIR to characterize the thermally treated products.[13] C, H, and N analyses were performed by Onieda Research Services, Inc., Whitesboro, NY, and X-ray fluorescence analyses for Fe were carried out on dimethyl sulfoxide solutions of 1 using an energy-dispersive EDAX EXAM-6 spectrometer. Cyclic voltammetry at 100 mV/s was performed in acetonitrile solution containing 0.1 M [n-Bu$_4$N]-[ClO$_4$] electrolyte in a conventional H cell with a platinum working electrode and Ag/AgCl reference electrode. All reported potentials are vs SCE. Voltammograms were recorded with a Princeton Applied Research 173/175 potentiostat/programmer. Thermal analyses were performed using a Du Pont Instruments 951 thermogravimetric analyzer and 910 differential scanning calorimeter. Rapid-scan Fourier transform IR (RSFTIR) spectra were taken by using apparatus previously described.[14] The molecular weight distribution was determined with a Du Pont LC850-FA size exclusion chromatography apparatus with four 300 × 7.8 mm i.d., 500-Å Ultrastyragel columns and 220-nm UV detector calibrated against conventional polystyrene standards. The solvent and carrier were tetrahydrofuran.

Results and Discussion

Crystal Structure. The molecular structure of 1 is essentially equivalent for both phases. The details of the structure of the α-phase have recently been independently reported;[7c] however, it was obtained at room temperature and lacks esd's, and we have summarized the comparative structural data in Table I. Atom labeling can be found in Figure 1. The fractional coordinates and anisotropic thermal parameters are located in Tables S2 and S4 for the α-phase and Tables S3 and S5 for the β-phase. The intermolecular angles are presented in Table S6.

For both phases the C_5N rings are in a chair conformation, the C_4 diacetylene moiety is linear, and the mol-

(11) O'Connor, C. J. *Prog. Inorg. Chem.* **1982**, *29*, 203.
(12) (a) Gebert, E.; Reis, A. H., Jr.; Miller, J. S.; Rommelmann, H.; Epstein, A. J. *J. Am. Chem. Soc.* **1982**, *104*, 4403. (b) Miller, J. S.; Dixon, D. A.; Calabrese, J. C.; Vazquez, C.; Krusic, P. J.; Ward, M. D.; Wasserman, E., Harlow, R. L. *J. Am. Chem. Soc.*, in press.
(13) Chase, B. *Microchim. Acta* **1987**, *3*, 81–91.
(14) Cronin, J. T.; Brill, T. B. *Appl. Spectrosc.* **1987**, *41*, 1147. Karpowicz, R. J.; Brill, T. B. *Appl. Spectrosc.* **1983**, *37*, 79.

Table I. Distances (angstroms) for the α- and β-Phases of 4,4′-(Butadiyne-1,4-diyl)bis(2,2,6,6-tetramethyl-4-hydroxypiperidin-1-oxyl), 1

atoms	α-phase	α-phase[a]	β-phase
Intramolecular Bonding Distances			
O(2)-N(13)	1.282 (7)	1.28	1.301 (7)
O(4)-N(23)	1.282 (7)	1.28	1.285 (7)
O(1)-C(10)	1.5448 (9)	1.41	1.450 (7)
O(3)-C(20)	1.432 (9)	1.41	1.421 (8)
N(13)-C(12)	1.516 (9)	1.50	1.504 (9)
N(13)-C(14)	1.489 (6)	1.50	1.460 (10)
N(23)-C(22)	1.490 (10)	1.49	1.539 (10)
N(23)-C(24)	1.506 (9)	*b*	1.481 (9)
C(1)-C(2)	1.20 (1)	1.18	1.226 (10)
C(1)-C(10)	1.47 (1)	1.50	1.421 (11)
C(2)-C(3)	1.38 (1)	1.39	1.391 (8)
C(3)-C(4)	1.20 (1)	1.19	1.176 (10)
C(4)-C(20)	1.49 (1)	1.52	1.531 (11)
C(10)-C(11)	1.52 (1)	1.51	1.569 (9)
C(10)-C(15)	1.53 (1)	1.53	1.513 (14)
C(11)-C(12)	1.52 (1)	1.48	1.543 (9)
C(12)-C(16)	1.51 (1)	1.53	1.489 (8)
C(12)-C(17)	1.52 (1)	1.55	1.542 (9)
C(14)-C(15)	1.55 (1)	1.48	1.548 (15)
C(14)-C(18)	1.53 (1)	1.57	1.512 (14)
C(14)-C(19)	1.52 (1)	1.56	1.528 (10)
C(20)-C(21)	1.52 (1)	1.50	1.549 (14)
C(20)-C(25)	1.52 (1)	1.53	1.478 (10)
C(21)-C(22)	1.53 (1)	1.51	1.519 (15)
C(22)-C(26)	1.53 (1)	1.58	1.516 (10)
C(22)-C(27)	1.52 (1)	1.52	1.548 (13)
C(24)-C(25)	1.53 (1)	1.49	1.527 (9)
C(24)-C(28)	1.53 (1)	1.53	1.549 (9)
C(24)-C(29)	1.52 (1)	1.55	1.525 (10)
Intermolecular Hydrogen-Bonding Distances			
O(1)···O(2)	2.835 (8)[c]	2.81	2.804[e]
O(2)···H(1)	1.70[c]		1.85[e]
O(3)···O(4)	2.757 (8)[d]	2.74	2.788[f]
O(2)···H(1)	1.72 (9)[d]		1.84[f]

[a] From ref 7c. [b] Not reported in ref 7c. [c] $x, {}^1/_2 - y, {}^1/_2 + z$. [d] ${}^1/_2 - x, y, {}^1/_2 + z$. [e] ${}^1/_2 + x, 1 - y, z$. [f] ${}^1/_2 + x, 2 - y, z$.

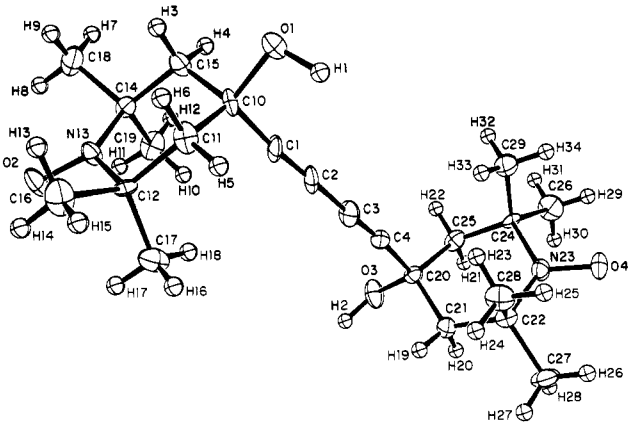

Figure 1. Atom labeling for 4,4′-(butadiyne-1,4-diyl)bis-(2,2,6,6-tetramethyl-4-hydroxypiperidin-1-oxyl), 1.

ecule as a whole possesses a nearly perfect noncrystallographic inversion center. Typical of diacetylenes,[8] the CC–CC separations average 1.38 and 1.391 Å and the average C≡C distances are 1.20 and 1.201 Å for the α- and β-phases, respectively. The average NO distances are 1.282 and 1.293 Å and the N's are essentially planar as the sum of the CNO and CNC angles average 357.7° for both the α- and β-phases. The intramolecular N···N distances are 10.113 and 10.123 Å for the α- and β-phases, respectively.

The packing motif is different for the two phases. In the α-phase the OH···ON hydrogen bonding interactions are 1.70 and 1.72 (9) Å and the O···O interactions are 2.834 (8) and 2.757 (8) Å.[15] The closest interdiacetylene separations range from 7.064 to 8.497 Å and on the basis of accepted structural criteria should not support single-crystal topochemical polymerization.[8] Adjacent parallel diacetylenes are separated by 14.113 Å. A stereoview of the α-phase can be found in Figure 2. There are two unique nitrogens per unit cell. The intermolecular N···N distances less than 9 Å are listed in Table II.

Table II. Intermolecular N•••N Distances (<9 Å) for the Two Unique Nitrogens

α-phase		β-phase	
N13	N23	N13	N23
5.612	5.612	5.272	5.272
6.400	6.400	6.261	6.261
6.542	6.542	6.384	6.384
7.216	7.206	7.396	7.348
7.251	7.216	7.518	7.348
7.251	7.409	7.396	7.518
7.409	7.437	7.608	7.608
7.437	7.833	7.620	7.620
7.706	8.381	8.079	8.079
8.112	8.451	8.079	8.079
8.451	8.538	8.508	8.508
8.659			
8.659			

The β-polymorph possesses well-separated diagonal chains knit together by OH···ON hydrogen bonding and forms corrugated sheets in the *ab* plane. The NO···HO distances are 1.84 and 1.85 Å and average 1.84 Å. The NO···O distances are 2.788 and 2.804 Å and average 2.796 Å. Thus, the α-phase has stronger hydrogen bonding as evidenced by the shorter separations. The closest C_4 diacetylenes separations are along the *b* axis and are C1···C4′ (5.19 Å), C2···C4′ (4.82 Å), and C3···C4′ (4.74 Å). Thus, like the α-phase, it should not support single-crystal topochemical polymerization.[8] Adjacent diacetylenes are essentially parallel and are separated by 10.083 ± 0.014 Å. A stereoview of the chair conformation of the monomer as well as the hydrogen-bonded knit structure is shown in Figure 3 for the β-phase. There are two unique nitrogens per unit cell. The intermolecular N···N distances less than 9 Å are listed in Table II.

Attempts to prepare an oligomer or polymer of **1** electrochemically failed. **1**, however, was characterized to possess a reversible two-electron (1.85 e^-) oxidation in acetonitrile at 0.77 V (vs SCE). This potential is consistent with oxidation processes for nitroxides.[16] In contrast, **3** exhibits a irreversible two-electron (1.96 e^-) oxidation at 0.67 V with concomitant precipitation on the electrode surface.

Magnetic Measurements. The molar magnetic susceptibility corrected for the diamagnetic core correction,[17] χ_M, and measured by the SQUID method at an applied field of 1 kG between 6 and 300 K was fit by the Curie–Weiss expression $\chi_M = C/(T - \theta)$, where the parameters are $\theta = -1.88$ K, $C = 0.74$ emu K/mol for α-phase and $\theta = -1.71$ K, $C = 0.73$ emu K/mol for β-phase, respectively, (Figure 4). These θ's are comparable to the −2 and −2.75 K values reported earlier for the α-phase by the Faraday technique.[7a,b] The SQUID-determined effective moment, μ_{eff}, is 1.73 μ_B per NO group, or 2.44 μ_B per molecule for α-phase and 1.71 μ_B per NO group or 2.41 μ_B per molecule for β-phase. These values are consistent with the Faraday measurements for two independent $S = {}^1/_2$ spins per

(15) Hamilton, W. C.; Ibers, J. A. *Hydrogen Bonding in Solids*; Benjamin: New York, 1968; p 16.
(16) Pokhodenko, V. D.; Platonova, E. P.; Kuts, V. S.; Radchenko, N. F. *Elektrokhimiya* **1984**, *20*, 1451–1456.
(17) The diamagnetic correction used was -259×10^{-6} emu/mol.

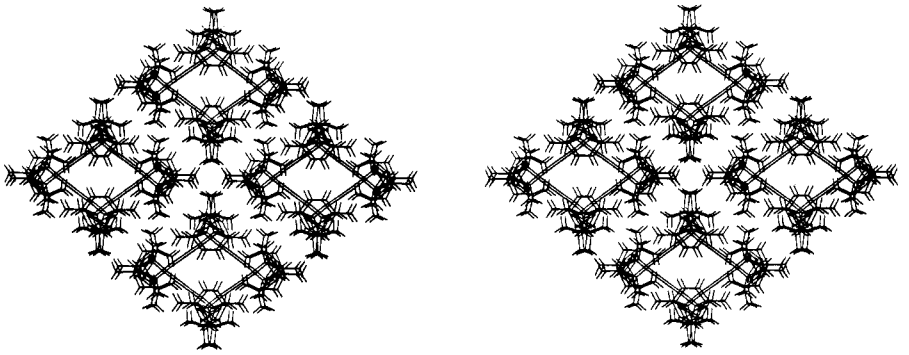

Figure 2. Stereoview of the *ab* plane of the α-phase of 4,4'-(butadiyne-1,4-diyl)bis(2,2,6,6-tetramethyl-4-hydroxypiperidin-1-oxyl), 1.

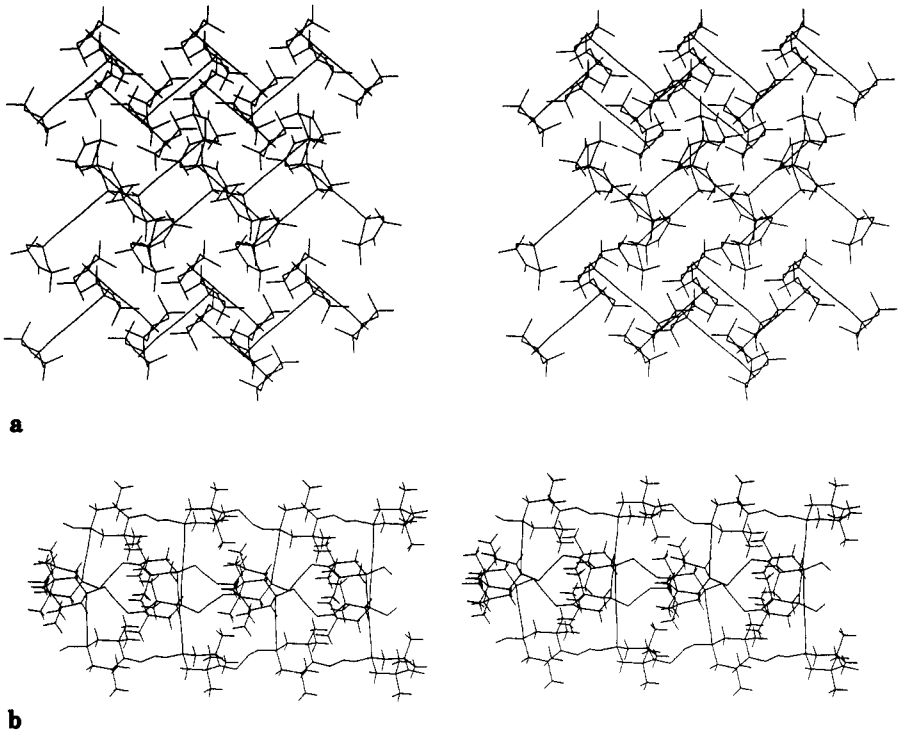

Figure 3. Stereoview of the of the β-phase of 4,4'-(butadiyne-1,4-diyl)bis(2,2,6,6-tetramethyl-4-hydroxypiperidin-1-oxyl), 1, along the *ab* (a) and *ac* planes (b).

molecule. For both phases, the magnetic moment is essentially temperature independent down to 20 K. These results have been independently reproduced by Faraday measurements at both Ohio State and Du Pont to temperatures as low as 2.1 K. The magnetic moment for both phases is reduced to 1.50 μ_B per NO group at 6 K due to a finite θ. The effective room-temperature moment is markedly larger than the 1.55 μ_B per monomer (or 1.10 μ_B per NO) reported earlier for the α-polymorph.[7b] Similar data are not reported by Cao and co-workers.[7d]

Measurement of the isotropic magnetic moment of 1 in deuterated methanol was carried out at 300 K using the Evans NMR method.[18a] Though subject to greater error,[18b] the observed moment of 2.25 μ_B is also consistent with two independent $S = {}^1/_2$ spins per molecule.

Careful analyses of the field-dependent magnetization (Honda analysis[12a]) for magnetic field up to 7.5 kG for several samples showed that ferromagnetic impurities are present in the range 10–30 ppm by weight of equivalent iron. The presence of iron was confirmed in both phases by using bulk X-ray fluorescence analysis on samples dissolved in dimethyl sulfoxide and was found to be in the 5–15-ppm range. At these levels there are many possible

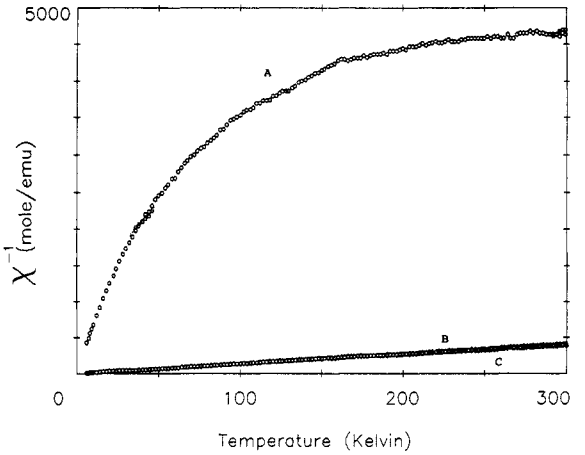

Figure 4. Reciprocal molar magnetic susceptibility, χ_M^{-1} as a function of temperature for heat-treated polycrystalline (A) α-phase and unheated (B) α- and (C) β-phases of 4,4'-(butadiyne-1,4-diyl)bis(2,2,6,6-tetramethyl-4-hydroxypiperidin-1-oxyl), 1.

(18) (a) Deutsch, J. L.; Poling, S. M. *J. Chem. Educ.* **1969**, *46*, 167. (b) O'Hare, D.; Green, J. C.; Chadwick, T. P.; Miller, J. S. *Organometallics* **1988**, *7*, 1335.

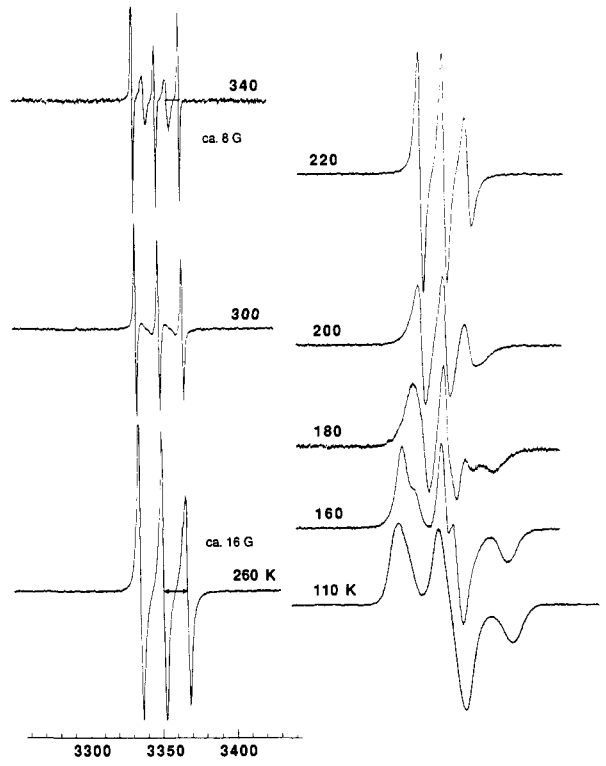

Figure 5. EPR spectrum of dilute (1.3×10^{-4} M) solution of 1 in deoxygenated EtOH solution at 110, 160, 180, 200, 220, 260, 300, and 340 K. All curves are to the same horizontal scale.

sources of contamination with ubiquitous iron in spite of several recrystallizations and care taken not to use metal utensils in handling and preparation. The most notable potential origins of ferromagnetic contamination include dust and iron impurities in the copper salts used in the acetylene coupling to prepare **2**.

Electron Spin Resonance. (a) Solution. The EPR studies of both α- and β-phases in dilute deoxygenated ethanol solution (1.3×10^{-4} M) provides insight into the magnetic couplings within this biradical material. At 200 K, the EPR spectrum, Figure 5, consists of three relatively sharp lines with a splitting of 16 G. This is in accord with the EPR expected for isolated monoradicals with a typical ^{14}N hyperfine interaction of aS_zI_z (S_z is the z component of the electron spin; I_z is the z component of the ^{14}N nucleus; a is the averaged hyperfine coupling constant, ~16 G[19]). At 200 K, the exchange interaction between the spins on either end of the biradical, JS_1S_2, is much smaller than the hyperfine interaction with each ^{14}N nucleus (i.e., $J \ll a$).[19a,20] With increasing temperature, a five-line EPR pattern emerges with 8 G separation (one-half the hyperfine splitting) between each line. The lines alternate in line width and intensity, as, for example, observed at 340 K (Figure 5). This is typical of a biradical system with $J \gg a$ and a time-dependent modulation of the exchange J.[21] A thermally activated weak exchange of this magnitude is typical of nitroxide biradicals such as diesters of tetramethylpiperidinoloxyl.[19a,20] The origin of this thermally activated exchange may involve thermal activated contribution of antibonding LUMOs enabling weak spin coupling or even indirect exchange via the solvent molecules. The rigid nature of the diacetylene bridge between the two nitroxides makes thermal activated flexing of the molecule and direct radical–radical interaction unlikely.

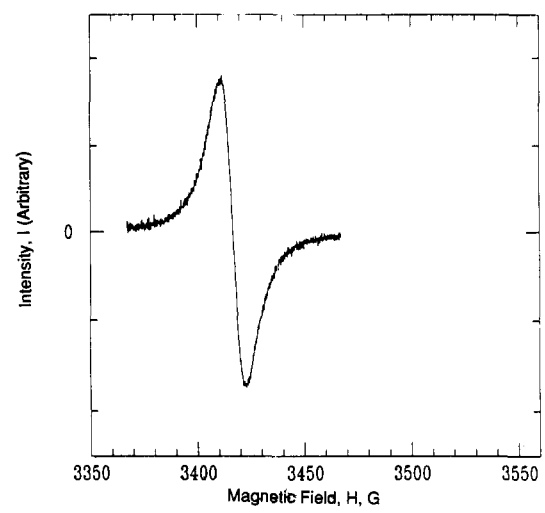

Figure 6. EPR spectrum of a crystal of β-phases of 1 at 290 K.

As the temperature of the solution decreases below the freezing point, the EPR pattern is transformed, for example, as observed at 110 K (Figure 5). The spectrum is now typical of an unoriented powder pattern for isolated nitroxide spins with slightly anisotropic g values and hyperfine interaction tensors (for orientations parallel and perpendicular to the molecular axes).[22] The peak-to-peak line width, ΔH_{pp}, may be accounted for by a combination of dipolar broadening due to neighboring protons and the other electron spin on the biradical. Assuming that the spin is somewhat delocalized from the NO moiety onto the neighboring carbon atoms, a dipolar field (H_{dip}^{proton}) ~9 G,[23] and that the dipolar field due to the radical at the opposite end of 1, $H_{dip}^{radical}$ {$\propto \mu_B/r^3$ [where r is the separation between the spin (i.e., N) sites, i.e., ~10 Å]} is ~9.3 G, then

$$\Delta H_{pp} = [(H_{dip}^{proton})^2 + (H_{dip}^{radical})^2]^{1/2} = 13 \text{ G}$$

which is in good agreement with the observed ΔH_{pp}. The narrower line widths for the similar spectra observed for the heat-treated samples (vide infra) supports that primarily monoradicals remain after heat treatment.

(b) Solid State. EPR studies of both α- and β-phases of the monomer gave nearly identical results. The EPR for the β-phase at 290 K is shown in Figure 6. The spectra consist of a single line with an integrated intensity varying as T^{-1}, in agreement with the temperature dependence of the static susceptibility. The ΔH_{pp} (~11 G) of the derivative spectrum and the line width at half-maximum intensity of the absorption spectrum, ΔH (~19.8 G), are temperature independent. ΔH may be used to extract the approximate interdiradical exchange interaction J assuming the Anderson and Weiss relationship for exchange narrowing:[24]

$$\Delta H_{exp} = g\mu_B(^{10}/_3 H_{dip}^2 + H_{hyperfine}^2)/J_{inter}[8S(S+1)]^{1/2}$$

where H_{hyp} is the hyperfine constant. Since the line width prevents the observation of hyperfine structure, we estimated it to be 20 G (value deducted from the pattern after

(19) (a) Glarum, S. H.; Marshall, J. H. *J. Chem. Phys.* **1967**, *47*, 1374. (b) Reitz, D. C.; Weissman, S. I. *J. Chem. Phys.* **1960**, *33*, 700. (c) Briere, R.; Dupeyre, R. M.; Lemaire, H.; Morat, C.; Rassat, A.; Rey, P. *Bull. Soc. Chim. Fr.* **1965**, 3290.

(20) Luckhurst, G. R. *Spin Labeling Theory and Applications*; Berlinger, L. S., Ed.; Academic Press: New York, 1976; p 133.

(21) Hudson, A.; Luckhurst, G. R. *Chem. Rev.* **1969**, *69*, 191.

(22) Poole, C. P.; Farach, H. A. *Theory of Magnetic Resonance*; Wiley-Interscience: New York, 1987; pp 313ff.

(23) Abragam, A. *Principle of Nuclear Magnetism*; Marshall, W. C., Wilkinson, D. H., Eds.; Oxford University Press: Oxford, 1961.

(24) Anderson, P. W.; Weiss, P. R. *Rev. Mod. Phys.* **1953**, *25*, 269.

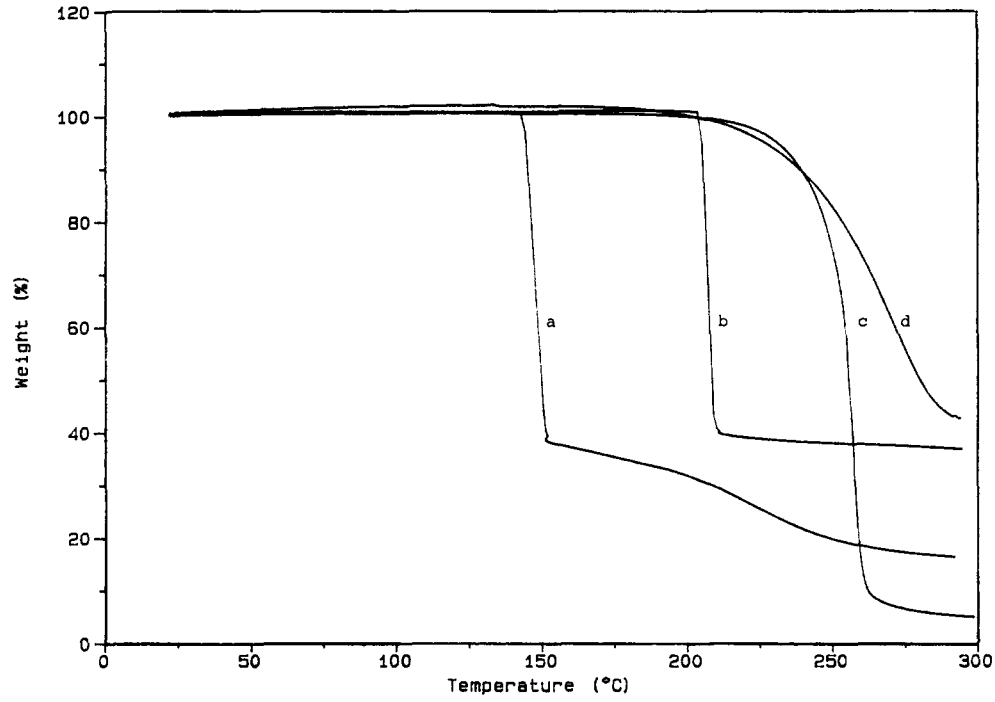

Figure 7. Thermogravimetric analysis of 4,4′-(butadiyne-1,4-diyl)bis(2,2,6,6-tetramethyl-4-hydroxypiperidin-1-oxyl), 1 (a), its dehydrated analogue 3, (b), and their bis(piperidine) precursors 2 (c) and 4 (d), respectively; 10 °C/min, 50 cm^3/min of N_2.

heat treatment, vide infra). H_{dipole} is a fluctuating dipolar field:[25]

$$H_{dipole} = [\sum_i \mu_B^2/r_i^6]^{1/2}$$

where r_i is the distance between the first N neighbors sites. Using the values of Table II, we found the average fluctuating dipole field to be ~136 and 141 G for the α- and β-phases, respectively. We estimated J_{inter} to be 0.155 K (~0.11 cm^{-1}) for the α-phase and J_{inter} 0.174 K (~0.12 cm^{-1}) for the β-phase. These values can be compared with those obtained independently from the molecular field expression[24] which gives an estimation of the exchange integral J^{WNF} as a function of $|\theta|$ as

$$^3/_2 k_B|\theta| = ZJ^{WMF}S(S+1)$$

where Z is the number of nearest neighbors and k_B is the Boltzmann constant. Using the experimentally measured (vide supra) $|\theta|$ of ~1.8 K for both phases together with $S = {}^1/_2$ and $Z = 22$ (for <8.6 Å), Table II, we estimate J^{WNF} ~ 0.160 cm^{-1} (~0.1 cm^{-1}). This is in good agreement with J_{inter} values. Inclusion of the contribution to H_{dip} of additional near neighbors in the calculation of J_{inter} would improve the agreement of the two independent estimates of the interradical exchange.

Thermal Treatment. The thermal reactions of 1–4 were studied by using thermal analysis and IR techniques as previously described.[14] Thermogravimetric (TGA) curves for these four compounds under the same conditions are shown in Figure 7, and several features become immediately apparent. First, given the structural similarities between the four compounds, it appears that the presence of the nitroxide group is a key factor in the relative stability of the compounds as both nitroxides decompose at lower temperatures than the piperidine compounds. Second, the hydroxyl functionality also appears to play a significant role since both hydroxylated compounds decompose at lower temperatures than their corresponding dehydrated

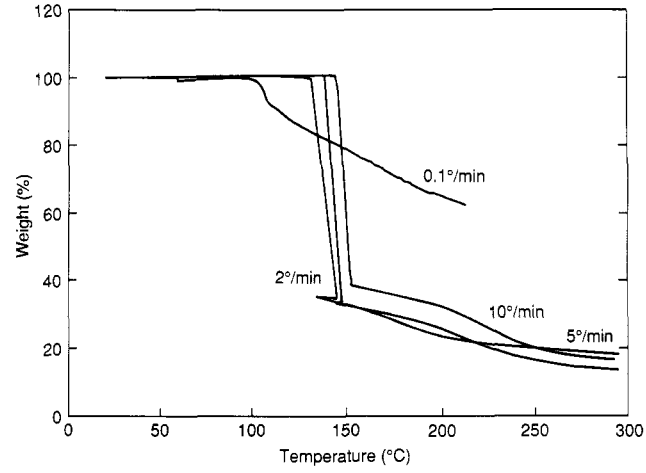

Figure 8. Thermogravimetric analysis of the β-phase of 4,4′-(butadiyne-1,4-diyl)bis(2,2,6,6-tetramethyl-4-hydroxypiperidin-1-oxyl), 1, at heating rates of 0.1, 2, 5, and 10 °C/min, 50 cm^3/min of N_2.

compounds. Although lower heating rates gave lower decomposition temperatures and less weight loss at equivalent temperatures as shown for the β-phase in Figure 8, both α- and β-phases had nearly identical behavior. Samples of both phases that had been powdered prior to analysis also gave essentially identical behavior; thus, no significant effects from differences in sample surface area were occurring.

Differential scanning calorimetry (DSC) under nitrogen shows the onset of a reaction between 60 and 80 °C followed by catastrophic decomposition at higher temperatures as indicated by the thermogravimetry. Isothermal calorimetry on the β-phase of 1 at 95 °C, Figure 9, shows that reaction occurs very slowly for the first hour or two, followed by increasingly rapid reaction which peaks at around 6 h. Reaction then rapidly decreases and is essentially complete after 7–8 h.

To gain a better understanding of these decomposition reactions and their relationship to the proposed polym-

(25) Pake, G. E.; Estle, T. L. *Electron Paramagnetic Resonance*; W. A. Benjamin Publishers: New York, 1973; p 157.

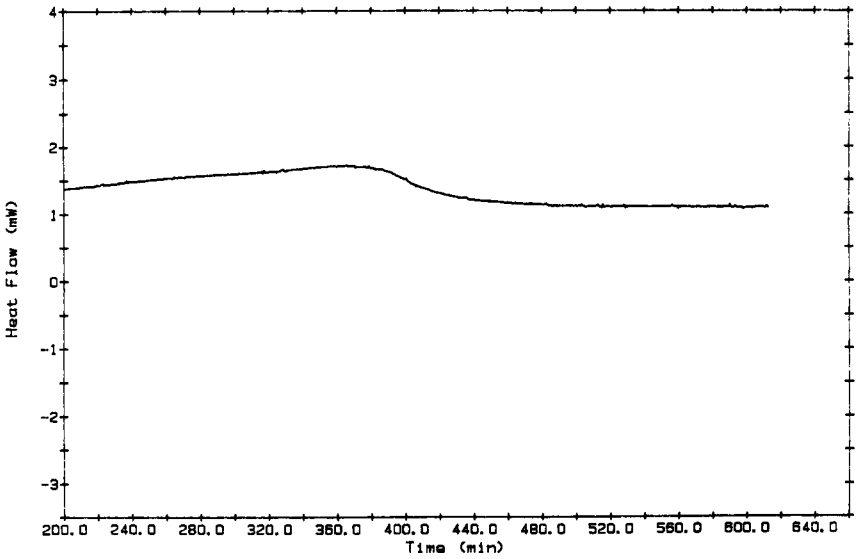

Figure 9. Isothermal (95 °C) differential scanning calorimetry of the β-phase of 4,4′-(butadiyne-1,4-diyl)bis(2,2,6,6-tetramethyl-4-hydroxypiperidin-1-oxyl), **1**, under N_2.

erization reaction, rapid-scan FTIR (RSFTIR) spectroscopy at relatively rapid heating rates often exposes features of the decomposition that become disguised at lower heating rates.[26] Since such a study requires detailed analysis of many spectra; only a summary of the results and conclusions will be presented here. The Raman and IR spectra of the α- and β-phase of **1** are nearly identical aside from subtle differences around 1170, 1300, and 1400 cm^{-1}, which may arise from the different hydrogen bonding or crystal packing (Figure 10). At a heating rate of 50 °C/s and 22 psi (abs) Ar pressure, both phases of **1** appear to decompose identically by RSFTIR, confirming the TGA results. Both samples decompose exothermically without melting at 190–200 °C to give CO, CO_2, methanol, and an unknown product absorbing at 890 cm^{-1}; no nitrogen-containing gaseous products were identified. The IR spectrum of the remaining solid residue is very similar to the spectra of **1** after slow heat treatment for extended periods of time. The α-phase of **1** was examined more carefully, and it was found that neither the heating rate (40–160 C/s) or Ar pressure (17–155 psi) had a significant effect on the products or their distribution. The decomposition temperature did not vary with pressure, but it increased with higher heating rates. This confirms the TGA results and suggests that an induction period is important as was shown by the isothermal DSC measurements.

Additional RSFTIR analyses on **2–4** show that only the nitroxides decompose with evolution of CO and CO_2 (in a ratio of ca. 3:1), while having a tertiary hydroxyl leads to the formation of methanol in the volatile decomposition products. Diradical **3** produces only a trace amount of methanol but along with its dehydrated precursor **4** produces methane as its major gas-phase product. These observations suggest that the nitroxide functionality is necessary for formation of CO and CO_2. The nitroxide likely acts as an oxygen donor since gas-phase NO products were not observed and in **2** is the only oxygen source. The results further suggest that the alkene functionality destabilizes the piperidine ring in **3** and **4** and results in methane formation, while in **1** and **2** it would seem likely that the ring breaks apart with loss of methanol. These

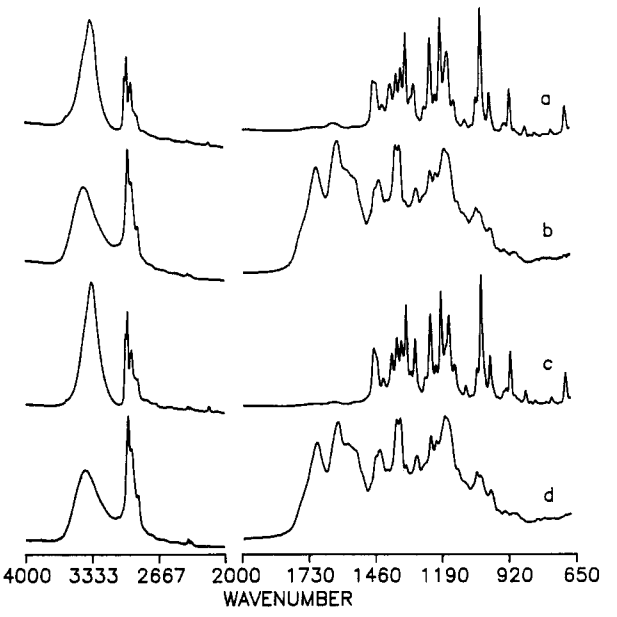

Figure 10. Transmission IR spectra of a neat polycrystalline film of the α- and β-phases of 4,4′-(butadiyne-1,4-diyl)bis(2,2,6,6-tetramethyl-4 hydroxypiperidin-1-oxyl), **1**, supported as KBr pellets (RT) and as a thin film supported between two NaCl plates (95 °C) before and after heating at 95 °C: (a) α-phase; (b) α-phase heated at 95 °C for 25 h; (c) β-phase; (d) β-phase heated at 95 °C for 25 h.

observations are important because *they lead us to conclude that in the thermolysis of* **1**, *reaction generally takes place with loss of the nitroxyl group (and the radical site) and destruction of the ring system.* Although these results do not preclude formation of some polymer or survival of some radical sites, they do show that the major reaction appears to be decomposition and should result in the formation of small molecules as products.

Solid-state decomposition processes were studied by FTIR on samples dispersed on NaCl plates and heated. Again both phases of **1** gave essentially identical solid products as did varying the thermal treatment (Figure 10). Most notably, the peak assigned to the nitroxide group at ca. 1340 cm^{-1} disappears with continued heating, the hydroxyl peak at ca. 3400 cm^{-1} decreases significantly, and the most dramatic changes occur in the 1550–1750-cm^{-1} region, where at least four peaks grow with sample de-

(26) Oyumi, Y.; Bill, T. B. *Combust. Flame* **1985**, *62*, 213. Brill, T. B.; Oyumi, Y. *J. Phys. Chem.* **1986**, *90*, 6848. Oyumi, Y.; Brill, T. B. *Propellants, Explos., Pyrotech.* **1988**, *13*, 69.

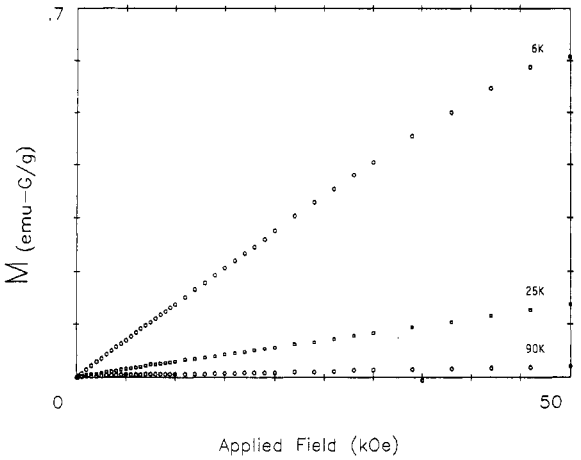

Figure 11. Field dependence of magnetization as a function of temperature for a heated sample of the α-phase.

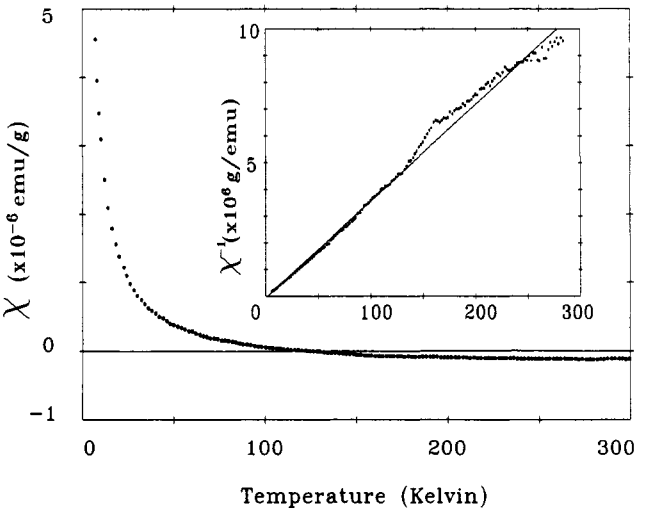

Figure 12. Gram magnetic susceptibility of ther heat-treated α-phase uncorrected for the diamagnetism of the constituent atoms plotted as a function of temperature. The inset contains the inverse gram susceptibility of the heat-treated α-phase corrected for molecular diamagnetism with $\chi_{dia} = -2.21 \times 10^{-7}$ emu/g. The line through the data points corresponds to the best fit of the Curie–Weiss law to the data ($C = 2.76 \times 10^{-5}$ emu/g), corresponding to ~0.15 of the initial number of spins remaining.

composition. These absorptions are likely due to the formation of C=O, C=N, N=O, and/or C=C bonds. Although Korshak et al. have suggested that the growth of absorptions in this region is consistent with polymerization of the diacetylene moiety and corresponds to C=C stretches in the polymer chain,[7b] the IR changes appear to be too dramatic and complex to be associated with a simple polymerization process.

These results led us to doubt the polymeric nature of 1 after heat treatment. The solubility of the thermolyzed materials was tested, and regardless of thermal treatment, the materials dissolved rapidly in solvents ranging in polarity from methylene chloride to methanol (samples dissolve essentially instantaneously in methanol) and exhibit partial solubility even in water or petroleum ether. Unfortunately, NMR spectra run on solutions of these materials were too complex to interpret. This type of behavior is unusual for polymers, especially polyconjugated materials, which are generally poorly soluble; thus, these materials are likely oligomeric.

To determine the molecular weight distribution of heat-treated samples of both the α- and β-phases, size exclusion chromatography was utilized. Both phases gave essentially equivalent results. The dominant peak with the greatest molecular weight had number- (and weight-) average molecular weights of 847 (915) and 685 (837) daltons for the α- and β-phases, respectively. This narrow distribution suggests approximate dimeric species are the largest species present in solution; however, there is evidence for a minor oligomeric fraction composed of 2–10 repeat units. The degree of polymerization may be somewhat higher, but at the expense of the desired nitroxyl side groups, leaving an oligomeric mixture. Even in the most optimistic view the molecular weights are not appreciable and the materials hardly warrant being called polymeric. Equal in intensity to the dimer peak is a peak with a molecular weight comparable to the monomer. This is consistent with thermal degradation of 1 to smaller molecular fragments.

Magnetic Measurements after Heat Treatment. The magnetic and EPR properties of both phases of 1 change drastically upon thermal treatment. The reciprocal magnetic susceptibility, χ^{-1}, is plotted in Figure 4, and the field dependence of the magnetization of the samples after thermal treatment measured at the temperatures of 6, 25, and 90 K in Figure 11. The details of the careful sample handling are described in the Experimental Section. The measured susceptibility, Figure 12, has considerable noise above 150 K due to only a very small amount of sample remaining in the bucket after heat treatment. After careful bucket correction is made, the field dependences of the magnetization do not show any evidence of existence of ferromagnetic behavior. If sufficient care is not exercised when converting the raw magnetic data to M(H), spurious results that imply ferromagnetic behavior may be obtained. The signals from the heat-treated materials that are being analyzed are very small as compared with the large diamagnetic contributions from the bucket, support wires, etc. The precision required by the experiments requires a correction for each individual data point by measuring the sample bucket under identical conditions. After extremely careful corrections were made, the spurious ferromagnetic signals disappeared and normal magnetic behavior was observed.

Magnetic-field-dependent studies at 2.2, 4.2, and 300 K were performed for samples thermally treated to temperatures as high as 85–90 °C for varying lengths of time up to 38 h both in sealed quartz tubes and under dynamic pumping. Honda analysis[12a] (plot of M_{expt}/H vs H^{-1}, where M_{expt} is the experimentally measured moment and H the applied magnetic field) of these samples failed to show any ferromagnetic component greater than the equivalent of 50 ppm Fe by weight, with more typical results in the range 30–50 ppm. Given the presence of 10–30 ppm by weight equivalent Fe in the monomer crystals (vide supra), these data are attributed to likely concentration of magnetic impurities during the destructive heat treatment. The temperature dependence of the susceptibility reflects the presence of typically one (independent) Curie spin per 15 monomer units after heat treatment.

Samples for EPR studies where heated at 85 °C under nitrogen for 96 h. The EPR spectra of both phases exhibit the same dramatic changes after heat treatment. A broad three-line pattern is observed even at room temperature (Figure 13), which is nearly identical with the spectrum of the frozen solution at 110 K (Figure 5). This reflects the nitrogen hyperfine interaction (from the pattern at 300 K we found H_{hyp} to be ~20 G). Comparison of the line width of this ESR spectrum can be compared to that of the frozen solution at 110 K, showing that for the heat-treated samples the ΔH_{pp} is narrower, i.e., ~11 G. This

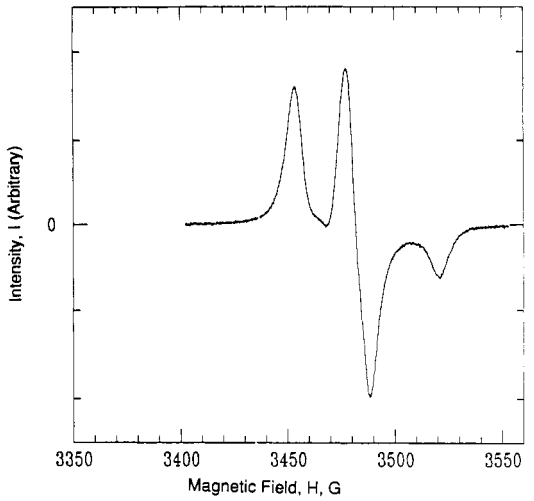

Figure 13. EPR spectrum of β-phase of 1 after heat treatment.

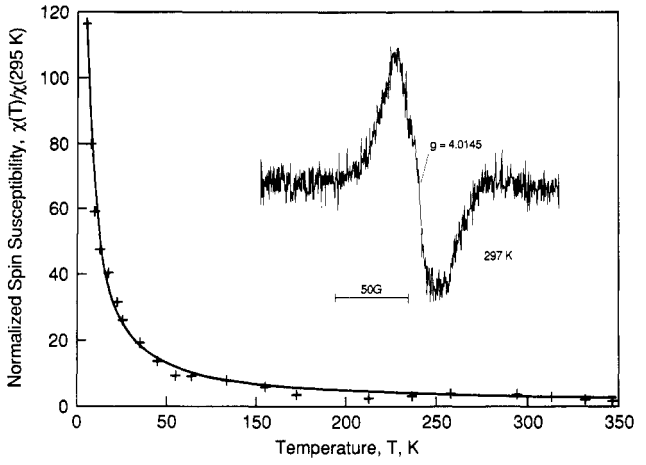

Figure 14. The 300 K EPR spectrum of the triplet signal from the heat treated β-phase of 1 (a). Temperature dependence of the triplet EPR signal (normalized to 1 at 295 K (b). The solid line is a fit to $I = C/T[3 + \exp(J/T)]$ with $J = 10$ cm^{-1}.

is consistent with the EPR line shape of the heat-treated samples being no longer broadened by dipolar interactions between the two spins of the diradical. These behaviors suggest that the large majority of the residual spins remaining after heat treatment are now monoradicals. This conclusion is in accord with the analysis of the vibrational spectra and essentially corroborate the static susceptibility measurements.

For both phases (before and after heat treatment) a very weak single line was observed at 300 K around 1700 G, e.g., Figure 14a for the β-phase, which may be due to the presence of an activated triplet state.[27] For this resonance the intensity temperature dependence, Figure 14b, was fitted to $I = C/T[3 + \exp(J/k_BT)]$ to yield an exchange interaction $J \sim +10$ K (~ 7 cm^{-1}). We were unable to observe additional signals at lower fields.[7a,b] Moreover, the absolute fraction of spins in the triplet state could not be readily estimated relative to the doublet since the triplet state is forbidden. The origin of the triplet line may be an impurity.

Radiative Treatment. Earlier reports in the literature claimed that 1 could be polymerized by exposure to light but radiation sources and polymerization conditions were not given.[7a,b] In an attempt to repeat these observations, both the α- and β-phases were exposed to UV visible light sources of varying wavelength and intensity and ^{60}Co γ and electron beam radiation as described in the Experimental Section. In no case was any type of polymerization or considerable change in the materials observed when the temperature was controlled to be lower than 60 °C. Darkening of the material was observed on prolonged UV exposure, but only after temperature control was removed. These results lead us to conclude that 1 is not photolytically active and earlier results may have been the result of uncontrolled thermal processes.

Conclusion

The 4,4′-(butadiyne-1,4-diyl)bis(2,2,6,6-tetramethyl-4-hydroxypiperidin-1-onyl), 1, diacetylene monomer is a well-behaved magnetic system composed of a pair of independent doublets without evidence for a significant triplet contribution. Since the spins on this diacetylene monomer couple only extremely weakly, it seems unlikely that should the desired single-crystal polymer form that it would possess spin coupling that could lead to high-spin or ferromagnetic behavior. A preferred model diacetylene monomer should have a spin-coupled triplet ground state as well as the ideal solid-state structure enabling topochemical polymerization.

The magnetic data of both phases of 1 as well as their thermal degradation products do not provide evidence that any polymeric or organic material present possesses ferromagnetic coupling or ferromagnetic behavior. Decomposition accompanied by concentration of ferromagnetic impurities in the reaction residue appears to adequately account for the slight increase in ferromagnetic properties observed upon thermolysis. These studies further suggest that, given the obvious complexity and dramatic nature of the decomposition processes, any nonmetallic ferromagnetic material that might be produced is likely to have ill-defined, variable, and poorly reproducible structures and properties and occur in such low yield that the method will be of little preparative value. Until such time as the alleged ferromagnetic component(s) of heat-treated 1 can be reproducibly synthesized and isolated in sufficient quantity to be unambiguously characterized as being organic, polymeric, and ferromagnetic, the claim that this material is a polymeric ferromagnet will be dubious.

Acknowledgment. A.J.E., D.T.G., R.L., P.V., and J. S.M. gratefully acknowledge partial support by the Department of Energy Division of Materials Science (Grant No. DE-FG02-86ER45271.A000). T.B.B. gratefully acknowledges support from the Air Force Office of Scientific Research, Aerospace Sciences (AFOSR-87-0033). We also thank R. Beckerbauer, B. Chase, P. J. Krusic, W. Marshall, M. Martin, R. S. McLean, S. Riggs, M. D. Ward and H. Williams assistance in these studies. C.J.O. acknowledges support from a grant from the Louisiana Education Quality Support Fund, administered by the Board of Regents of the state of Louisiana, and the donors of the Petroleum Research Fund, administered by the American Chemical Society.

Registry No. 1, 14306-88-8; 2, 78151-30-1; 3, 42325-52-0; 4, 78151-31-2; 5, 53654-26-5; 6, 69971-65-9.

Supplementary Material Available: Tables of crystallographic parameters, fractional coordinates, isotropic and anisotropic thermal parameters, and bond angles of 4,4′-(butadiyne-1,4-diyl)bis(2,2,6,6-tetramethyl-4-hydroxypiperidin-1-oxyl), 1 (14 pages); calculated and observed structure factors for the α- and β-phases of 1 (14 pages). Ordering information is given on any current masthead page.

(27) Atherton, N. M. *Electron Spin Resonance*; Halsted Press: New York 1973; p 150.